Development of a metabolomics-based data analysis approach for identifying drug metabolites based on high-resolution mass spectrometry

Development of a metabolomics-based data analysis approach for identifying drug metabolites based on high-resolution mass spectrometry

Hsiao-Hsien Ting [a,1], Yi-Shiou Chiou [b,1], Tien-Yi Chang [c], Guan-Yu Lin [d], Pei-Jhen Li [d,*], Chia-Lung Shih [c,**]

[a] Department of Anesthesiology, Ditmanson Medical Foundation Chia-Yi Christian Hospital, Chia-Yi City 60002, Taiwan
[b] Master Degree Program in Toxicology, College of Pharmacy, Kaohsiung Medical University, Kaohsiung 80756, Taiwan
[c] Clinical Research Center, Ditmanson Medical Foundation Chia-Yi Christian Hospital, Chia-Yi City 60002, Taiwan
[d] Department of Chemistry and Biochemistry, National Chung Cheng University, Chiayi 621301, Taiwan

Abstract

A metabolomics-based approach to data analysis is required for drug metabolites to be identified quickly. This study developed such an approach based on high-resolution mass spectrometry. Our approach is a two-stage one that combines a time-course experiment with stable isotope tracing. Pioglitazone (PIO) was used to improve glycemic management for type 2 diabetes mellitus. Consequently, PIO was taken as a model drug for identifying metabolites. During Stage I of data analysis, 704 out of 26626 ions exhibited a positive relationship between ion abundance ratio and incubation time in a time-course experiment. During Stage II, 25 isotope pairs were identified among the 704 ions. Among these 25 ions, 18 exhibited a dose-response relationship. Finally, 14 of the 18 ions were verified to be PIO structure-related metabolite ions. Otherwise, orthogonal partial least squares-discriminant analysis (OPLS-DA) was adopted to mine PIO metabolite ions, and 10 PIO structure-related metabolite ions were identified. However, only four ions were identified by both our developed approach and OPLS-DA, indicating that differences in the designs of metabolomics-based approaches to data analysis can result in differences in which metabolites are identified. A total of 20 PIO structure-related metabolites were identified by our developed approach and OPLS-DA, and six metabolites were novel. The results demonstrated that our developed two-stage data analysis approach can be used to effectively mine data on PIO metabolite ions from a relatively complex matrix.

Keywords: A time-course experiment, OPLS-DA, Pioglitazone, Stable isotope tracing

1. Introduction

Drug metabolism investigations are a key part of the drug discovery process [1]. Liquid chromatography—mass spectrometry (LC/MS) is an analytical technique for profiling drug metabolism. Due to advances in LC/MS technology, high-resolution LC/MS has sufficient sensitivity for detecting trace compounds [2]. Thus, several metabolomics-based approaches to data analysis have been established for rapid drug metabolite identification with high-resolution LC/MS [3−5], such as the mass defect filter (MDF) [6], XCMS Online [7], stable isotope tracing [8], and orthogonal partial least squares-discriminant analysis (OPLS-DA) [9]. However, the metabolites identified among these various analytical approaches are inconsistent, and a lot of non-target metabolite ions are identified by these approaches [5]. Therefore, the development of a metabolomics-based data analysis is necessary to effectively and comprehensively identify drug metabolites.

Time-course experiments have been widely adopted to investigate cellular processes or pharmacokinetics

[5,10]. In a time-course experiment for liver enzyme incubation with drugs, drug metabolite levels increased with incubation time. Therefore, we designed a metabolomics-based approach to data analysis to identify drug metabolites in a time-course experiment. According to previous study, a lot of endogenous compounds significantly differ in their relative concentrations between dose groups and were identified by some metabolomics-based data analysis approaches, such as XCMS Online [11]. To improve the efficacy of our approach, we added stable isotope tracing for metabolite identification [4,12]. Through stable isotope tracing, isotope pairs of metabolite ions can be identified from liver enzyme incubation using native- and isotope-labeled drugs [13]. Our previous study demonstrated that the use of MDF with stable isotope tracing improves the efficacy of metabolite identification [13]. Thus, we inferred that a time-course experiment with stable isotope tracing can also improve the efficacy of metabolite identification.

The OPLS-DA has been widely adopted to identify biomarkers or metabolites from tissues, urine, or plasma based on high-dimensional data, such as MS data [5,14–16]. This approach has also been used to successfully identify toxic metabolites, and the efficacy of OPLS-DA in identifying metabolites has been relatively high [5]. Therefore, we adopted the OPLS-DA as a form of multivariable statistical analysis to differentiate between two groups using high-dimensional data and to identify key features. Additionally, differences in metabolite identification between our approach and the OPLS-DA could be assessed.

Pioglitazone (PIO) is a thiazolidinedione drug that is used to improve glycemic control among patients with type 2 diabetes mellitus [17]. The reported side effects of PIO include hepatotoxicity cases and fulminant hepatic failure [18–20]. The ring opening in thiazolidinedione has been linked to reactive metabolites of thiazolidinedione drugs [21]. The ring-opening metabolites of PIO were first reported in dog microsomes [22] and were subsequently found in rat and human microsomes [23]. However, the LC/MS resolution adopted by them was low [22,23] and some PIO metabolites have yet to be discovered. Recently, PIO metabolism has been investigated using high-resolution LC/MS, and the MDF technique was adopted to identify metabolite ions [13]. Although the MDF technique is also one of the metabolomics-based data analytical approaches for drug metabolite identification, but the metabolites identified were limited to the mass defect window (50 mDa) and mass change window (50 Da) relative to that of the parent drug, its core fragment templates, or its conjugate templates [3]. Although

many novel PIO structure-related metabolite ions (11 ions) were identified by MDF using a high-resolution LC/MS [13], some novel PIO metabolites beyond the ranges set in MDF could be identified using non-targeted metabolomics-based data analysis approaches. Thus, PIO was taken as a model drug in this study, and its metabolites were identified using our developed data analysis approach.

The study developed a metabolomics-based data analysis approach for drug metabolite identification using high-resolution LC/MS. We developed a two-stage data approach using a time-course experiment and stable isotope tracing. Moreover, we investigated differences in metabolite identification by comparing our approach with the OPLS-DA. We expected that our developed approach could be effectively used to identify drug metabolites.

2. Material and methods

2.1. Study design

The study design is illustrated in Fig. 1. First, two sample sets of liver enzyme incubations of PIO were prepared for our approach and OPLS-DA. The incubation samples were analyzed by LC/MS to produce the MS files. The MS files were converted to peak lists, and the two data analysis approaches were adopted to mine possible drug metabolite ions from these peak lists respectively. A dose–response experiment was conducted to validate probable PIO metabolite ions. Finally, these validated ions were further analyzed for having a PIO structure-related ion using LC-MS/MS analysis. The procedure is detailed in the following sections.

2.2. Chemicals

Glucose-6-phosphate dehydrogenase (activity: 225 units/mg), $MgCl_2$ (purity: $\geq 98\%$), D-glucose 6-phosphate disodium salt hydrate (purity: $\geq 98\%$), sulfatase (activity: 11 units/mL), β-glucuronidase (activity: >85000 units/mL), sodium phosphate monobasic monohydrate (purity: $\geq 98\%$), β-nicotinamide adenine dinucleotide phosphate sodium salt hydrate (NADP, purity: $\geq 98\%$), sodium phosphate dibasic (purity: $\geq 99\%$), and acetic acid (purity: $\geq 99\%$) were obtained from Sigma–Aldrich (St. Louis, MO, USA). PIO (purity = 97%), deuterium-labeled rosiglitazone (purity = 98%), and deuterium-labeled (on the benzene ring) PIO (D_4-PIO, purity = 97%) were obtained from Toronto Research Chemicals (Toronto, Canada). Human liver S9 fractions (20 mg/mL protein base) were obtained from Thermo Fisher Scientific (Runcorn, UK).
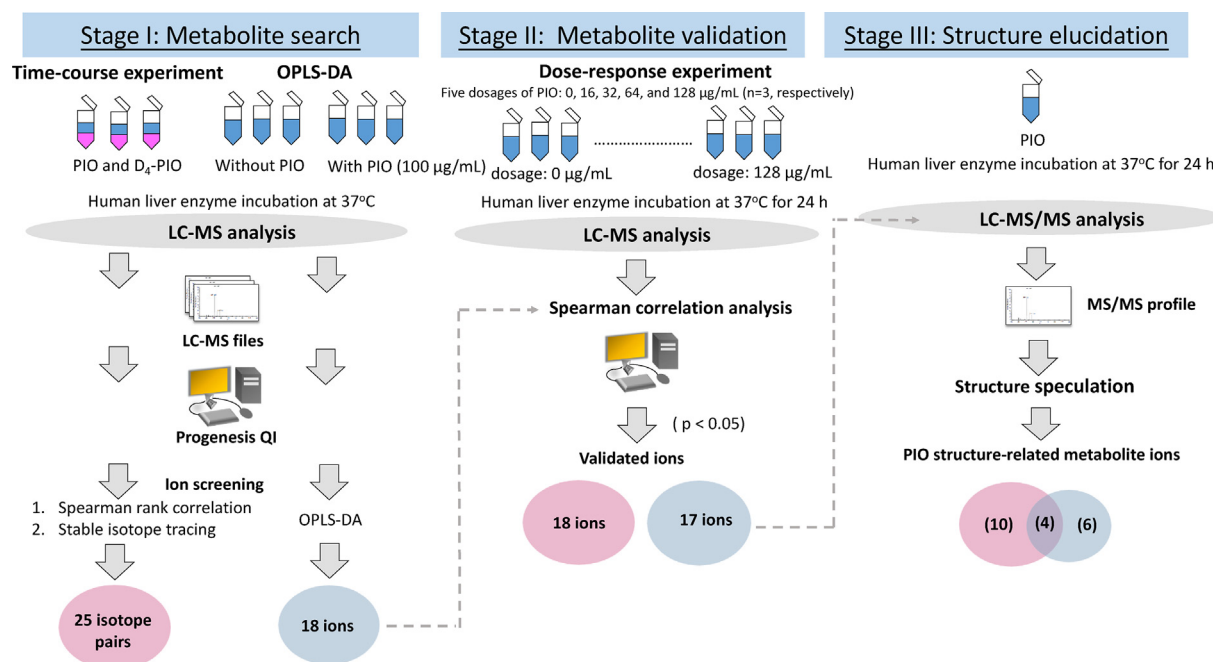
Fig. 1. Overview and flowchart of the developed method and the currently proposed method for drug metabolite identification. In stage I, metabolite candidates were identified by using two methods, respectively. In stage II, these identified metabolite candidates were further validated by dose—response experiment. In stage III, the chemical structures of these validated metabolites were elucidated based on LS-MS/MS analysis.

2.3. Human liver S9 incubation

Human liver S9 fractions were incubated with PIO for producing metabolites. The 0.5 mL mixture consisted of 1 mM NADP, 3 mM $MgCl_2$, 06 U mL^{-1} glucose 6-phosphate dehydrogenase, 3 mM glucose 6-phosphate, and 3.75 mg mL^{-1} human liver S9 fractions, and 0.5 μ/mL parent drugs (PIO and D_4-PIO) in phosphate buffer (100 mM and pH 7.4). The mixture was incubated at 37 °C in a bath incubator for 24 h, then incubated at 37 °C for 90 min with β-glucuronidase (13 μL) and sulfatase (5 μL) for deconjugation, followed by having 28 μL of 20% acetic acid (v/v) in deionized water added to terminate enzyme reactions. To adjust the run-to-run variance from the LC/MS analysis, 10 μL of D_3-rosiglitazone (1000 ppb) was added to the mixture. To extract supernatants, the mixture was centrifuged for 10 min at 13500 rpm. Next, these supernatants were filtered using a 0.22 μm PVDF membrane filter (MSonline Scientific Co., Ltd. Taiwan). Then, the filtered samples were then extracted with C18 solid-phase extraction cartridges (Sep-Pak C18 1 cc Vac Cartridge, 50 mg sorbent per cartridge, 55—105 μm) that had been pre-conditioned with 2 mL methanol and 2 mL 1% acetic acid (v/v) in deionized water. Finally, the filtered sample was transferred to the cartridges, which were then washed with 2 mL of 1% acetic acid (v/v) in deionized water and analytes were eluted with 1 mL of methanol.

2.4. LC/MS and LC-MS/MS

A total of 5 μL incubation sample was injected into the LC/MS system, which included an Orbitrap Fusion Lumos Tribrid Mass Spectrometer (Thermo Fisher Scientific, San Jose, CA, USA) in which an electrospray ion source and an UltiMate 3000 HPLC system were used. With a resolution of 120 000, the mass scan range was adjusted to an m/z 80 to 800. An electrospray ionization (ESI)-MS analysis was conducted with an ion-spray voltage of 3500 V in the positive ion ESI mode. LC separation was carried out using an ACQUITY UPLC BEH C18 Column (2.1 mm × 100 mm, 1.7 μm). The mobile phase solvents comprised deionized water mixed with 0.1% formic acid (A) and methanol mixed with 0.1% formic acid (B) with a linear gradient elution at a flow rate of 300 μL/min. The following profile was used to execute the elution program: 0—1 min, 99% solvent A; 1—1.01 min, 1—50% solvent B; 1.01—7 min, 50—99% solvent B; 7-8 min, 99% solvent B; 8-8.01min, 99% solvent A; and 8.01-10min 99% solvent A. For the LC-MS/MS analysis, the parameters were the same as in the LC/MS analysis, and a collision energy of 30, 35, or 40 eV was used to generate precursor fragments.

2.5. Time-course experiment combined with stable isotope tracing

In a time-course experiment, PIO and D_4-PIO (100 μg/mL) were incubated with human liver S9 fractions for 0, 2, 4, and 6 h ($n = 3$ for each time point). The procedure for liver enzyme incubation is described in Section 2.2. Subsequently, these incubation samples were analyzed using LC/MS to produce raw MS files, and these files were then converted to peak lists using Progenesis QI software (Nonlinear Dynamics, Newcastle, UK) without any limitations (including retention time (RT) window, peak intensity, and charge state), and the peak lists included *m/z* values, RTs, charge states, and raw abundance. To adjust the run-to-run variance resulted from the LC/MS analysis, the raw abundance was divided by the abundance of spiked sample standard (D_3-rosiglitazone) to produce the peak abundance ratios, which were used for further analysis. During Stage I of the data analysis approach, Spearman rank correlation was adopted to estimate the correlation between abundance ratios and incubation time for each ion in the time-course experiment. A correlation coefficient (R) > 0.7 and a P value of <0.001 were considered a PIO metabolite candidate ion. Among the ions identified as candidates, some were PIO and D_4-PIO metabolite ions. During Stage II, the stable isotope tracing technique was used to identify isotope pairs from these candidate ions; a mass difference of 4.025 ± 0.001 Da, an RT shift within 0.1 min, and charge state = 1 were adopted when mining data on the isotope pairs.

2.6. OPLS-DA

For the use of OPLS-DA, two groups with different dosages were prepared. For one group, PIO (100 μg/mL) was incubated with liver enzyme. For the other group, no PIO was incubated in the liver enzyme. Six incubation samples were evaluated in each group using LC/MS to produce MS files. The MS files were converted to peak lists by Progenesis QI software. These abundances were normalized by dividing these by the abundance of the spiked sample standard, and the abundance ratios were used in further statistical analyses. The peak lists of two groups were analyzed using OPLS-DA, and PIO metabolite candidate ions were selected based on S-plots (p (corr) [1] > 0.5 and p [1] > 0.5). OPLS-DA was performed using MetaboAnalyst 5.0 (https://www. metaboanalyst.ca/).

2.7. Dose−response experiment

The levels of drug metabolites were expected to be correlated positively with drug concentrations. Therefore, we designed a dose−response experiment to validate the identified ions as possible PIO metabolite ions. PIO samples at five dosages (0, 16, 32, 64, and 128 μg/mL; n = 3, respectively) were incubated with human liver S9 fractions. The procedure for liver enzyme incubation is described in Section 2.2. The samples were analyzed using LC/ MS to produce MD files, and the MS files were converted to peak lists by Progenesis QI. These ion abundances were divided by the abundance of the spiked sample standard to obtain normalized ion abundances. The Spearman rank correlation between normalized peak abundances and the expected PIO dosages were estimated. An ion with a P-value <0.05 was considered as a validated metabolite ion. All statistical analyses were performed using R software (version 4.1.0, http://r-project.org/).

2.8. Chemical structure elucidation

These ions exhibited a dose-response relationship were adopted for structure elucidation. Several strategies were adopted to propose the structures of the novel ions. The possible structures of these ions were searched from online databases, such as HMDB, PubChem, Metlin, and Chemspider [24]. This strategy was used to identify already known metabolites. Otherwise, the known biotransformation routes were adopted to propose structures of the identified ions [24]. If the above-mentioned strategies could not be used to propose structures, we manually proposed the structures based on elemental formula and annotated fragment ions. Finally, these proposed structures were *in silico* fragmented by using CFM-DI [25,26], and the proposed structures could be confirmed by comparing the predicted and experimental fragment patterns. Mass errors (between the predicated and experimental fragment ions) < 5 ppm were considered as the same ion. The structures of fragment ions were determined based on the results of CFM-DI. All of structures were correctly drawn by using ChemDraw software version 20.1. The confidence level of structure elucidation was estimated based on the guideline [27].

3. Results and discussion

This study developed a new metabolomics-based data analysis approach for mining data on drug

metabolites. The two-stage data analysis approach mined PIO metabolite ions in MS data, including using a time-course experiment and stable isotope tracing. Additionally, OPLS-DA was used to mine data on drug metabolites as a comparison. These identified ions were validated as possible PIO metabolite ions using a dose−response experiment. Finally, employing LC-MS/MS analysis, these validated ions were determined to be PIO structure-related metabolite ions.

3.1. Mining data on PIO metabolite ions from LC-MS findings (Stage I)

A time-course experiment for the human liver enzyme incubation of PIO and D_4-PIO was prepared. The incubation samples generated PIO and D_4-PIO metabolites, and the levels of these metabolites increased with incubation time. The samples were analyzed using LC-MS for producing full-scan MS files. Progenesis QI software was used to transform the MS files into peak lists, and a total of 26626 ions were obtained. During Stage I of data analysis approach, the Spearman rank correlation was adopted to estimate the correlation between ion abundance ratios and incubation time in the time-course experiment. An ion with $R > 0.7$ and $P < 0.001$ was considered a PIO metabolite candidate ion, and a total of 704 metabolite candidate ions were identified. Among these possible metabolite ions, some were paired ions with isotopes. During stage II, the stable isotope tracing technique was used to mine isotope-paired ions from the 704 ions, and 25 paired ions (with a mass change $= 4.025 \pm 0.001$, an RT shift <0.1 min, and a charge state $= 1$) were identified.

The OPLS-DA was also adopted as a comparison for mining data on PIO metabolite ions. The MS files of the two groups (dosage $= 0$ and 100 μg/mL, respectively) were converted into peak lists, and a total of 25926 ions were collected. These ion abundance ratios of two groups were analyzed using the OPLS-DA, and the score plot (Fig. 2) indicates that the two groups were well-separated with a cumulative R^2X of 0.459, R^2Y of 0.968, and Q^2 of 0.945 for cross-validation (Fig. 2). The model was not over-fitted because the values were higher than the recommended values of 0.5, except for R^2X [28]. The S-plot of the OPLS-DA was adopted to determine crucial ions that were significantly different between the two groups. Two variables were used to draw the S-plot: p (corr) [1] and p [1] (Fig. 2). The variable of p (corr) [1] indicated the Pearson correlation coefficient between ion abundance ratios and the sample scores. The samples with higher dosages scored higher in the OPLS-DA. The ions with a higher p (corr) [1] value have abundance ratios that are associated with dosage. The other variable p [1] is the covariance between the ion abundance ratios and the sample scores. A larger covariance indicates a greater change in ion abundance ratios between the two groups. An ion with higher p (corr) [1] and p [1] values should be a PIO metabolite ion with high possibility. Thus, PIO metabolite candidate ions are displayed in the top-right corner of the S-plot. A total of 18 candidate ions were selected based on the self-determined criteria (p (corr) [1] > 0.5 and p [1] > 0.5) (Fig. 2).

3.2. Metabolite validation (Stage II)

The candidate ions identified by metabolomics-based approaches to data analysis may not be target metabolite ions [5,11]. Alternative methods to validate the identified ions are necessary. Drug metabolites should have a dose-response relationship; consequently, a dose−response experiment was conducted to validate metabolite ions as possible target metabolites [4]. Consequently, we conducted this experiment to validate the ions identified by our approach. Among the 25 ions identified by our approach, 18 ions exhibited a dose-response relationship (Table 1). Among the 18 ions identified by OPLS-DA, 17 ions exhibited a dose-response relationship (Table 2). These validated signals were further analyzed for structure elucidation.

3.3. Structure elucidation (Stage III)

Structure elucidation of the identified ions is a way with high level of evidence to confirm if they are drug metabolites. Although the use of synthetic standards is the best method for determining the structure of identified ions, it costs much time and money. Alternatively, MS/MS product ion profiles indicating the ion structure can be used to initially determine whether the identified ions are drug metabolites [5]. If the speculated structure resembles a component of the parent drug, it may be a drug metabolite.

The incubation samples were analyzed using LC-MS/MS to determine the MS/MS product ion profiles of the validated ions. Among the 18 ions identified using our approach, the structures of 14 ions could be inferred (Fig. S1 (https://nam11.safelinks.protection.outlook.com/?url=https%3A%2F%2Fwww.jfda-online.com%2Fcgi%2Fviewcontent.cgi%3Ffilename%3D3%26article%3D3425%26context%3Djournal%26type%3Dadditional&data=05%7C01%7Cn.kamaraj%40elsevier.com%7C751e92bc6cf54859ea3108dac7eb595e%
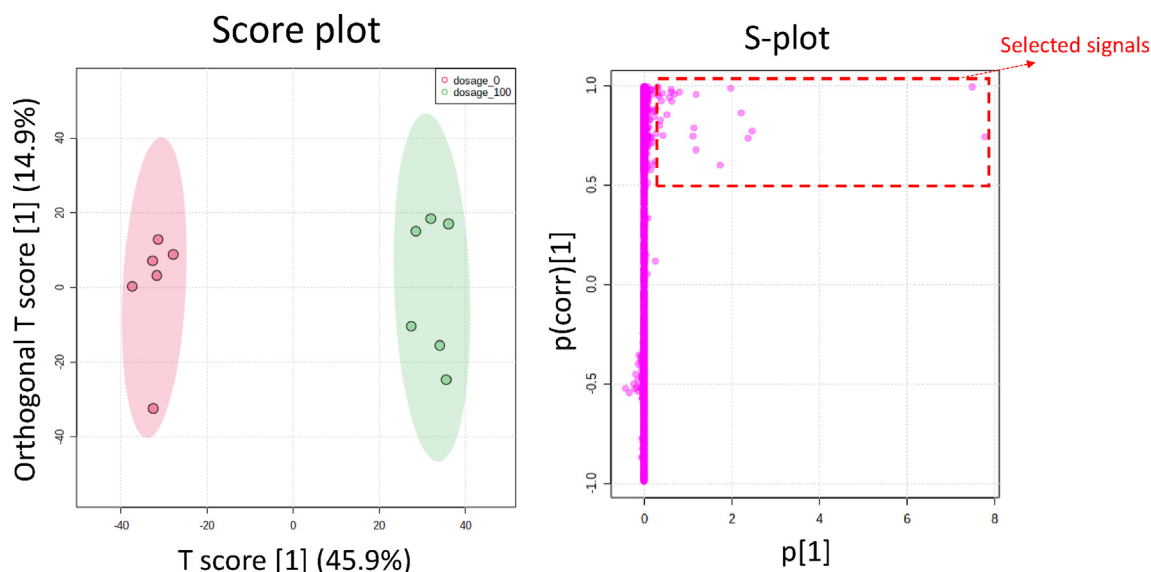
Fig. 2. Score plot (left side) and S-plot (right side) obtained from OPLS-DA.

7C9274ee3f94254109a27f9fb15c10675d%7C0%7C0%
7C638042110900320617%7CUnknown%7CTWFpb
GZsb3d8eyJWIjoiMC4wLjAwMDAiLC
JQIjoiV2luMzIiLCJBTiI6Ik1haWwiLCJXVCI6Mn0%
3D%7C3000%7C%7C%7C&sdata=r87Sssg3b6Db
DyO3xOXRlfQPI6pyUaxchvvduWYlmOA%
3D&reserved=0)). Among the 17 ions identified
using OPLS-DA, the structures of 10 ions could be
inferred (Fig. S1 (https://nam11.safelinks.protection.
outlook.com/?url=https%3A%2F%2Fwww.jfda-
online.com%2Fcgi%2Fviewcontent.cgi%3Ffilename
%3D3%26article%3D3425%26context%3Djournal%
26type%3Dadditional&data=05%7C01%7Cn.
kamaraj%40elsevier.com%7C751e92bc6cf54859ea

3108dac7eb595e%7C9274ee3f94254109a27f9fb15c
10675d%7C0%7C0%7C638042110900320617%
7CUnknown%7CTWFpbGZsb3d3eyJWIjoiMC4w
LjAwMDAiLCJQIjoiV2luMzIiLCJBTiI6Ik
1haWwiLCJXVCI6Mn0%3D%7C3000%7C%7C%
7C&sdata=r87Sssg3b6DbDyO3xOXRlfQPI6py
UaxchvvduWYlmOA%3D&reserved=0)).   These
inferred structures may be metabolized from PIO
(Fig. S1 (https://nam11.safelinks.protection.outlook.
com/?url=https%3A%2F%2Fwww.jfda-online.com
%2Fcgi%2Fviewcontent.cgi%3Ffilename%3D3%
26article%3D3425%26context%3Djournal%26type%
3Dadditional&data=05%7C01%7Cn.kamaraj%
40elsevier.com%7C751e92bc6cf54859ea3108
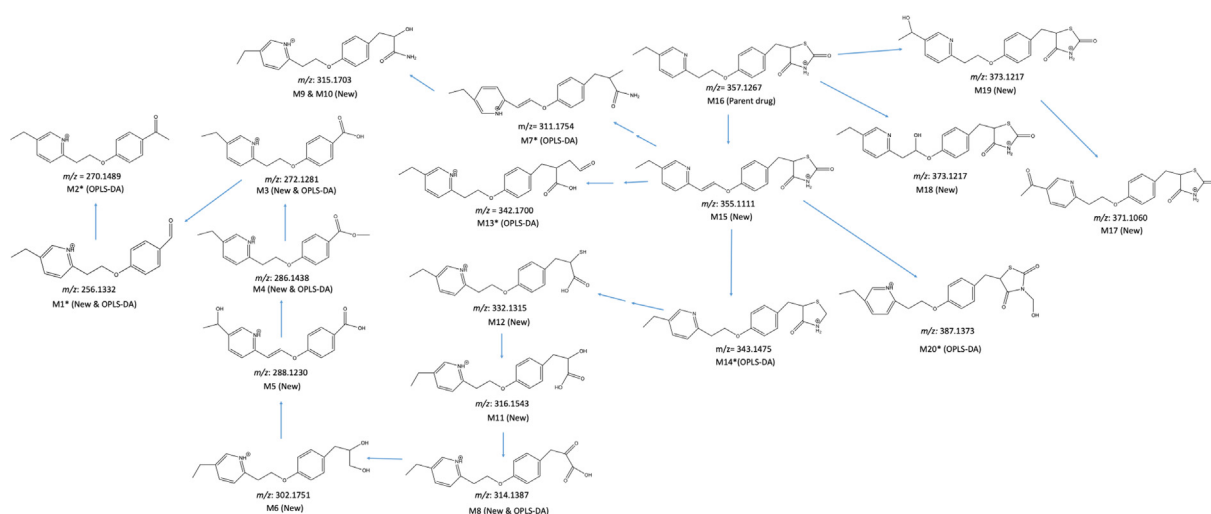
Fig. 3. Proposed PIO metabolite ions identified by our approach (new) and OPLS-DA and their possible metabolic pathways. Stars indicate novel PIO metabolite ions. Arrows indicate possible metabolic pathways.

Table 1. Major characteristics of PIO metabolite ion candidates identified by the developed approach.

ID	Ion		Isotope pair		Charge state	Mass difference[b]	R[c]	p-value[c]
	m/z	RT[a]	*m/z*	RT[a]				
1	256.1331	3.79	260.1582	3.78	1	−4.025	0.98	<0.001
2	272.1280	3.69	276.1531	3.68	1	−4.025	0.95	<0.001
3	286.1437	3.65	290.1687	3.64	1	−4.025	0.98	<0.001
4	288.1229	3.40	292.148	3.40	1	−4.025	0.83	<0.001
5	302.1749	3.65	306.2001	3.64	1	−4.025	0.99	<0.001
6	314.1386	3.39	318.1636	3.39	1	−4.025	0.93	<0.001
7	315.1702	3.15	319.1953	3.15	1	−4.025	0.87	<0.001
8	315.1702	3.35	319.1953	3.34	1	−4.025	0.98	<0.001
9	316.1542	3.49	320.1794	3.49	1	−4.025	0.90	<0.001
10	318.0980	3.51	322.1231	3.50	1	−4.025	0.84	<0.001
11	331.1651	3.18	335.1901	3.18	1	−4.025	NA	NA
12	332.1314	3.51	336.1565	3.49	1	−4.025	0.98	<0.001
13	355.1109	4.56	359.136	4.54	1	−4.025	0.74	0.003
14	371.1058	4.65	375.1309	4.64	1	−4.025	0.81	0.001
15	371.1058	4.02	375.1309	4.01	1	−4.025	NA	NA
16	373.0851	4.38	377.1102	4.37	1	−4.025	NA	NA
17	373.1214	3.92	377.1465	3.91	1	−4.025	0.73	0.003
18	373.1215	4.59	377.1466	4.57	1	−4.025	0.77	0.001
19	373.1215	3.62	377.1464	3.61	1	−4.025	0.73	0.003
20	378.1190	4.94	382.1439	4.92	1	−4.025	0.96	<0.001
21	387.1007	3.63	391.1258	3.63	1	−4.025	0.39	0.173
22	389.1163	3.42	393.1414	3.42	1	−4.025	NA	NA
23	395.1034	3.62	399.1285	3.61	1	−4.025	NA	NA
24	467.1301	3.32	471.1552	3.31	1	−4.025	NA	NA
25	479.1301	3.82	483.1552	3.81	1	−4.025	0.79	0.001

[a] Retention time.
[b] Mass difference between ion and its isotope pair.
[c] Spearman correlation coefficients obtained from the dose−response experiment and the corresponding *P* values. NA: not available.

Table 2. Major characteristics of PIO metabolite ion candidates identified by the OPLS-DA.

ID	*m/z*	RT[a] (min)	RT window (min)	Mass	Charge state	R[b]	p-value[b]
1	256.1331	3.75	0.23	255.1258	1	0.98	<0.001
2	270.1488	3.85	0.14	269.1415	1	0.95	<0.001
3	272.1280	3.66	0.13	271.1207	1	0.95	<0.001
4	286.1437	3.62	0.29	285.1364	1	0.98	<0.001
5	311.1753	3.63	0.13	310.168	1	0.95	<0.001
6	314.1386	3.37	0.21	313.1313	1	0.93	<0.001
7	330.1160	5.12	0.28	658.2174	2	0.98	<0.001
8	331.1235	5.07	0.30	660.2325	2	0.97	<0.001
9	331.1236	5.15	0.22	660.2326	2	NA	NA
10	342.1699	3.92	0.15	341.1626	1	0.98	<0.001
11	343.1474	3.86	0.15	342.1401	1	0.95	<0.001
12	347.1097	5.34	0.33	692.2048	2	0.86	<0.001
13	357.1267	3.88	0.24	356.1194	1	0.90	<0.001
14	378.1191	4.87	0.15	377.1119	1	0.96	<0.001
15	387.1372	3.60	0.14	386.1299	1	0.98	<0.001
16	406.1317	3.20	0.21	405.1244	1	0.93	<0.001
17	509.1409	3.74	0.15	508.1336	1	0.88	<0.001
18	528.1507	4.63	0.21	527.1435	1	0.97	<0.001

[a] Retention time.
[b] Spearman correlation coefficients obtained from the dose−response experiment and the corresponding *P* values. NA: not available.

dac7eb595e%7C9274ee3f94254109a27f9fb15c10675d%7C0%7C0%7C638042110900320617%7CUnknown%7CTWFpbGZsb3d8eyJWIjoiMC4wLjAwMDAiLCJQIjoiV2luMzIiLCJBTiI6Ik1haWwiLCJXVCI6Mn0%3D%7C3000%7C%7C%7C&sdata=r87Sssg3b6D

bDyO3xOXRlfQPI6pyUaxchvvduWYlmOA%3D&reserved=0)), because they possessed specific ion fragments (*m/z* 134.0964 and *m/z* 150.0913) commonly observed in PIO metabolites [29]. Thus, these ions should be considered as PIO structure-

Table 3. Major characteristics of PIO structure-related metabolite ions identified by our approach and OPLS-DA.

ID	*m/z*	RT[a] (min)	Charge state	Major fragment ion	Formula	Mass error (ppm)	R[b]	p-value[b]	Literature[c]	Method[d]	Confidence level[e]
M1	256.1331	3.79	1	134.10	$C_{16}H_{17}NO_2$	−0.51	0.93	<0.001		New approach&OPLS_DA	Level 3
M2	270.1488	3.85	1	134.10	$C_{17}H_{19}NO_2$	−0.50	0.95	<0.001		OPLS-DA	Level 3
M3	272.1280	3.69	1	134.10	$C_{16}H_{17}NO_3$	−0.35	0.98	<0.001	[13]	New approach&OPLS_DA	Level 3
M4	286.1437	3.65	1	134.10	$C_{17}H_{19}NO_3$	−0.52	0.90	<0.001	[13]	New approach&OPLS_DA	Level 3
M5	288.1229	3.40	1	134.10, 150.10	$C_{16}H_{17}NO_4$	−0.34	0.60	0.025	[13]	New approach	Level 3
M6	302.1749	3.65	1	134.10, 270.15	$C_{18}H_{13}NO_3$	−0.50	0.74	0.002	[13]	New approach	Level 3
M7	311.1753	3.63	1	134.10, 294.15	$C_{19}H_{22}N_2O_2$	−0.32	0.95	<0.001		OPLS-DA	Level 3
M8	314.1386	3.39	1	134.10, 270.15	$C_{18}H_{19}NO_4$	−0.46	0.78	0.001	[13]	New approach&OPLS_DA	Level 3
M9	315.1702	3.35	1	134.10	$C_{18}H_{22}N_2O_3$	−0.38	0.92	<0.001	[13]	New approach	Level 3
M10	315.1702	3.14	1	134.10, 270.15	$C_{18}H_{22}N_2O_3$	−0.24	0.93	<0.001	[13]	New approach	Level 3
M11	316.1542	3.49	1	134.10, 270.15	$C_{18}H_{21}NO_4$	−0.18	0.90	<0.001	[13]	New approach	Level 3
M12	332.1314	3.51	1	134.10	$C_{18}H_{21}NO_3S$	−0.37	0.80	0.001	[29]	New approach	Level 3
M13	342.1699	3.92	1	134.10, 298.18	$C_{20}H_{23}NO_4$	−0.28	0.98	<0.001		OPLS-DA	Level 3
M14	343.1474	3.86	1	134.10	$C_{19}H_{22}N_2O_2S$	−0.24	0.95	<0.001		OPLS-DA	Level 3
M15	355.1109	4.56	1	134.10, 284.11	$C_{19}H_{18}N_2O_3S$	−0.47	0.95	<0.001	[13]	New approach	Level 3
M16	357.1267	3.88	1	134.10	$C_{19}H_{20}N_2O_3S$	−0.09	0.90	<0.001	[29]	OPLS-DA	Leve1 3
M17	371.1058	4.65	1	148.08	$C_{19}H_{18}N_2O_4S$	−0.63	0.81	0.001	[30]	New approach	Level 1
M18	373.1215	4.59	1	150.09	$C_{19}H_{20}N_2O_4S$	−0.64	0.63	0.016	[13]	New approach	Level 3
M19	373.1215	3.62	1	132.08, 150.09 355.11	$C_{19}H_{20}N_2O_4S$	−0.61	0.75	0.002	[13]	New approach	Leve1 3
M20	387.1372	3.60	1	134.10, 357.13	$C_{19}H_{22}N_2O_4S$	−0.36	0.98	<0.001		OPLS-DA	Leve1 3

[a] Retention time.
[b] Spearman correlation coefficients obtained from the dose−response experiment and the corresponding *P* values.
[c] The metabolite ions identified by the literature.
[d] The ions were identified by our developed approach (named new approach) or OPLS-DA.
[e] The confidence level of structural identification was based on the guideline [25].

related metabolite ions. A total of 20 PIO structure-related metabolites were identified using either our approach or OPLS-DA, and four metabolites were identified in both approaches. The major characteristics of these 20 ions are illustrated in Table 3, and the measurement of the mass of these identified ions were highly accurate (mass error <1 ppm), as indicated in comparisons against their expected m/z values.

A total of 14 identified ions (M3, M4, M5, M6, M8, M9, M10, M11, M12, M15, M16, M17, M18, and M19) were previously reported PIO metabolites based on their m/z values [13,29,30]. Eleven of them (M3, M4, M5, M6, M8, M9, M10, M11, M15, M18, and M19) were identified by our previously reported study [13] based on their m/z values (mass error <5 ppm), RTs (RT shift within 1 min), and MS/MS profiles. Their chemical structures were further confirmed by using CFM-DI. For the proposed structures of M3, M4, and M9, one *in-silico* generated fragment ion at m/z 134.0964 was found in their experimental MS/MS profiles. For the proposed structures of M5, M18, and M19, one *in-silico* generated fragment ion at m/z 150.0913 was found in their experimental MS/MS profiles. For the proposed structures of M6, M8, M9, and M11, two *in-silico* generated fragment ions at m/z 134.0964 and m/z 270.1489 were found in their experimental MS/MS profiles. For the proposed structure of M15, two *in-silico* generated fragment ions at m/z 134.0964 and m/z 284.1104 were found in the experimental MS/MS profile. We found that only one or two fragment ions of the experimental MS/MS profiles could match *in-silico* generated fragment ions. Otherwise, M12, M15, and M17 were identified in the previous reports [29,30]. The reported four fragment ions of M12 (m/z 119, 132, 270, and 286) were found in our experimental M/MS profile. M16 was a PIO, and the reported fragment ions (m/z 119.07, 134.10, 116.08, 241.14, 286.12, and 314.12) were identified in our experimental MS/MS profile [29]. The reported fragment ions of M17 (m/z 148 and 254) were identified by our experimental MS/MS profile [30]. Thus, the chemical structures of M12, M16, and M17 could be confirmed.

The six novel ions (M1, M2, M7, M13, M14, and M20) were searched in the databases based on m/z value, positive ionization mode, mass tolerance (5 ppm), and MS/MS profile. However, no known chemicals were matched. Moreover, these ions were not from the common biotransformation m/z changes from PIO. Finally, the structures of these ions were manually proposed by annotation of their MS/MS profiles. The structures were proposed based on elemental formula and annotated fragment ions. These proposed structures were further

confirmed by using CFM-ID. For the proposed structures of M1 and M2, one *in-silico* generated fragment ion at m/z 134.0964 was found in their experimental MS/MS profiles. For the proposed structure of M7, two *in-silico* generated fragment ions at m/z 134.0964 and 294.1489 were found in its experimental MS/MS profile. For the proposed structure of M13, two *in-silico* generated fragment ions at m/z 134.0964 and 298.1802 were found in its experimental MS/MS profile. For the proposed structure of M14, three *in-silico* generated fragment ions at m/z 134.0964, 298.1260, and 326.1209 were found in its experimental MS/MS profile. For the proposed structure of M20, three *in-silico* generated fragment ions at m/z 134.0964, 286.1260, and 357.1267 were found in its experimental MS/MS profile. These proposed structures of novel ions seem to be reasonable.

The possible pathways of these novel metabolites were inferred based on the known enzymatic reactions [3,31,32] (Fig. 3). The m/z value of M1 was 256.1331 that was 15.9949 amu less than that of M3. The major fragment ion of M1 was observed at m/z 134.0964 which was similar to that of M3 (Fig. S1 (https://nam11.safelinks.protection.outlook.com/?url=https%3A%2F%2Fwww.jfda-online.com%2Fcgi%2Fviewcontent.cgi%3Ffilename%3D3%26article%3D3425%26context%3Djournal%26type%3Dadditional&data=05%7C01%7Cn.kamaraj%40elsevier.com%7C751e92bc6cf54859ea3108dac7eb595e%7C9274ee3f94254109a27f9fb15c10675d%7C0%7C0%7C638042110900320617%7CUnknown%7CTWFpbGZsb3d8eyJWIjoiMC4wLjAwMDAiLCJQIjoiV2luMzIiLCJBTiI6Ik1haWwiLCJXVCI6Mn0%3D%7C3000%7C%7C%7C&sdata=r87Ssg3b6DbDyO3xOXRlfQPI6pyUaxchvvduWYlmOA%3D&reserved=0)). The possible pathway of M1 was that the carboxyl acid group of M3 was reduced to an aldehyde group. The m/z value of M2 was 270.1489 that was 1.9792 amu less than that of M3. M2 and M3 had the same major fragment ion (m/z 134.0964). Thus, the possible pathway of M2 was that the ketone group of M2 was oxidized to the carboxyl acid group of M3. The m/z value of M7 was 311.1754 that was 3.9949 amu less than that of M9/M10. M7 had a unique fragment ion (294.1489) that was different from those of M9/M10, indicating that the structure of M7 had benzylic dehydrogenation. The possible pathway of M7 was that M9/M10 was from M7 via hydroxylation and desaturation. The m/z value of M13 was 342.1700 that was 14.9567 amu less than that of PIO. M13 had a unique fragment ion (m/z 298.1802) that was different from that of PIO. The proposed structure of this fragment ion had a thiazolidinedione ring-opening, indicating

that M13 was a thiazolidinedione ring-opening metabolite. The possible pathways from PIO to M13 may include reduction, hydration, and carboxylation. The *m/z* value of M14 was 343.1475 that was 13.9792 amu less than that of PIO. M14 had one fragment ion with a thiazolidinedione ring (*m/z* = 326.1210), indicating that M14 had a stable structure with a thiazolidinedione ring. The possible pathway of M14 was that the ketone group of PIO on the thiazolidinedione ring was reduced to a methyl group. The *m/z* value of M20 was 387.1373 that was 30.0106 amu greater than that of PIO. One fragment ion of M20 was PIO, indicating that the possible pathway of M20 was from PIO via adding methanol. The other fragment ion was observed at *m/z* 134.0964, indicating that methanol didn't add on the alkyl side chain of pyridine. Thus, the possible structure of M20 was that methanol added on the thiazolidinedione ring.

To determine whether our approach can be used to identify PIO metabolites, the inferred structure of M17 was synthesized by the Department of Chemistry and Biochemistry, National Chung Cheng University, Taiwan, based on the synthetic procedure of the Tanis group [33]. The synthetic standard (200 ppb) was analyzed by LC/MS and LC-MS/MS. The results demonstrated that M17 and the synthetic standard eluted at a similar RT (M17 at 4.62 min and the standard at 4.64 min) (Table S2 (https://nam11.safelinks.protection.outlook.com/?url=https%3A%2F%2Fwww.jfda-online.com%2Fcgi%2Fviewcontent.cgi%3Ffilename%3D3%26article%3D3425%26context%3Djournal%26type%3Dadditional&data=05%7C01%7Cn.kamaraj%40elsevier.com%7C751e92bc6cf54859ea3108dac7eb595e%7C9274ee3f94254109a27f9fb15c10675d%7C0%7C0%7C638042110900320617%7CUnknown%7CTWFpbGZsb3d8eyJWIjoiMC4wLjAwMDAiLCJQIjoiV2luMzIiLCJBTiI6Ik1haWwiLCJXVCI6Mn0%3D%7C3000%7C%7C%7C&sdata=r87Sssg3b6DbDyO3xOXRlfQPI6pyUaxchvvduWYlmOA%3D&reserved=0)) and had the same major ion fragment (*m/z* 148.0754) (Table S2 (https://nam11.safelinks.protection.outlook.com/?url=https%3A%2F%2Fwww.jfda-online.com%2Fcgi%2Fviewcontent.cgi%3Ffilename%3D3%26article%3D3425%26context%3Djournal%26type%3Dadditional&data=05%7C01%7Cn.kamaraj%40elsevier.com%7C751e92bc6cf54859ea3108dac7eb595e%7C9274ee3f94254109a27f9fb15c10675d%7C0%7C0%7C638042110900320617%7CUnknown%7CTWFpbGZsb3d8eyJWIjoiMC4wLjAwMD AiLCJQIjoiV2luMzIiLCJBTiI6Ik1haWwiLCJXVCI6Mn0%3D%7C3000%7C%7C%

7C&sdata=r87Sssg3b6DbDyO3xOXRlfQPI6pyUaxchvvduWYlmOA%3D&reserved=0)). These results indicates that the inferred structure of M17 was correct. Thus, our approach could be used to identify PIO metabolites.

PIO has been linked to the production of harmful metabolites in the human body [29]. The toxicity of PIO has been connected to thiazolidinedione ring-opening metabolites [29]. Our previous report identified nine novel thiazolidinedione ring-opening metabolites [13]. Among the six novel PIO structure-related metabolites identified in this study, four of them (M1, M2, M7, and M13) were thiazolidinedione ring-opening metabolites. Up to date, several thiazolidinedione ring-opening metabolites of PIO have been identified by using high-resolution LC/MS; however, the toxicity of the metabolites requires further research.

3.4. Our developed approach

In this study, we attempted to develop a metabolomics-based data analysis approach for drug metabolite identification. A time-course experiment combined with stable isotope tracing was designed to mine drug metabolite ions from MS data. In the time-course experiment, several ions (n = 704) demonstrated a positive relationship between ion abundance ratios and incubation time when the criteria were set as $R > 0.7$ and $P < 0.001$. Although stricter criteria were set for mining data on PIO metabolite ions, the same ions (704 ions for $R > 0.8$ and a P value < 0.001) were also identified. The number of ions that exhibited a positive relationship was unexpected. We inferred that the levels of several endogenous metabolites in the incubation samples increase with incubation time. The endogenous metabolites may have been affected by PIO metabolites; consequently, we identified many non-target metabolite ions during Stage I of data analysis. A time-course experiment can effectively filter out 97% of interference ions (25,922/26,626), but many still remain. Thus, the inclusion of an additional approach that removes these interference ions is necessary.

Stable isotope tracing has been designed to mine metabolite ions [4,12]. A complex statistical procedure was adopted in that stable isotope tracing for improving the efficacy of metabolite identification. However, only a few metabolites (4—5 ions) could be verified as structure-related metabolite ions [4,12]. The statistical procedure may have been overly complex, leading to only a few ions fulfilling the predetermined criteria [4].

To overcome this problem, we designed a simpler method in stable isotope tracing for drug metabolite identification. In stable isotope tracing, only the differences in mass (4.025 Da) between ions with a relatively small RT (RT shift <0.1 min) were adopted to mine isotope pairs from the metabolite candidate ions. Our results demonstrated that this stable isotope tracing technique could effectively identify 25 isotope pairs from the 704 ions identified in the time-course experiment. Finally, 14 of them could be verified as PIO structure-related metabolite ions, indicating that our two-stage data analysis approach could effectively mine data on drug metabolites.

3.5. Our approach versus OPLS-DA

OPLS-DA is a multivariable statistical analysis and can be used to discriminate between two groups with high-dimensional data using key features from MS data. Two dosage groups were prepared for the OPLS-DA, and the selected features were considered possible drug metabolite ions. Our results demonstrated that the OPLS-DA was an effective approach for drug metabolite identification; 10 of the selected 18 ions were verified as PIO structure-related metabolite ions. Among the 10 ions, four ions were identified by our approach (Fig. 4), indicating an inconsistency between different metabolomics-based data analysis approaches in terms of the metabolite ions identified.

We expected that our approach could identify all possible PIO metabolite ions. For comparison, the OPLS-DA to mine data on major metabolites, and only PIO metabolite ions with a relatively high abundance could be identified. Thus, we expected that our approach could identify all the metabolite

ions identified by the OPLS-DA. However, the identified metabolite ions were inconsistent between the two approaches, and only 4 out of 10 ions identified by the OPLS-DA could be identified using our approach. We designed our approach to mine data on ions that exhibited a positive relationship between ion abundances and incubation time. By contrast, the OPLS-DA was used more effective in mining data on ions that clearly differed in ion abundance between the two dosages. Most PIO structure-related metabolite ions (M2, M7, M13, M14, and M20) were identified by the OPLS-DA but could not be identified by our approach. None of these ions (M2, M7, M13, M14, and M20) exhibited a positive relationship between abundance ratios and incubation time in the time-course experiment. Therefore, some metabolite ions had an abundance that significantly differed between the two dosages but exhibited no positive relationship between abundance ratio and incubation time. This is one limitation in our approach for identifying metabolites. A more comprehensive approach should be developed for drug metabolite identification in the future.

3.6. Our developed approach versus MDF

Our previous report adopted MDF to mine PIO metabolite ions using high-resolution LC/MS [13]. MDF is commonly used to mine drug metabolites. Additionally, the experimental process of MDF is similar to our approach and warranted a comparison. MDF was used to mine those common PIO metabolites that were within the MDF window of 50 mDA and the mass change window of 50 Da relative to that of PIO [13]. A total of 13 PIO structure-related
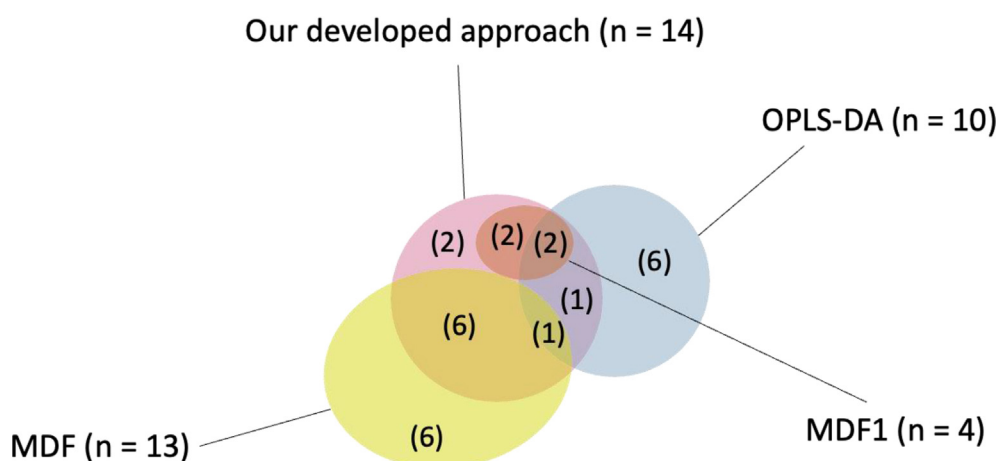

Fig. 4. Overlap of the PIO structure-related metabolites identified by different metabolomics-based data-processing approaches. MDF (mass defect filter) and MDF1 (mass change over the window of 50 Da) were adopted to identify PIO metabolites in our previous report [13]. Numbers in brackets indicates the number of identified PIO structure-related metabolite ions.

metabolite ions were identified by MDF and four uncommon PIO structure-related metabolite ions were identified by MDF1 (change in mass over the window of 50 Da). Although, we expected our approach to be capable of identifying these 13 ions, only 7 out of the 13 ions (M8, M9, M10, M11, M15, M18, and M19) were identified using our approach (Table 3 and Fig. 4).

In Step II, a dose—response experiment was conducted to validate the identified ions in our approach, but a time-course experiment was conducted for the MDF technique [13]. As mentioned, some levels of metabolite ions were positively correlated with PIO dosages but were not correlated with incubation time. As expected, six PIO structure-related metabolite ions were identified by MDF but not by our approach could be identified in Stage I of data analysis. Consistent with expectations, five ions (m/z 331.1651 at RT 3.19 min, m/z 371.1058 at RT 4.03 min, m/z 373.1214 at RT 3.92 min, m/z 387.1007 at RT 3.63 min, and m/z 389.1163 at RT 3.42 min) were identified in Stage I (Table 1).

Theoretically, the two ions (M12 and M17) identified by our approach can also be identified by MDF (Table 3), but this was not the case. Because MS data were converted into peak lists by Progenesis QI, we did not set any limitations in generating ions in our approach. However, the ions with a intensity less than 0.001% of the most intensity ion were excluded in MDF to reduce the number of possible interference ions [13]. These two ions (M12 and M17) might be excluded during the data conversion procedure in MDF. For uncommon metabolites (mass change window >50 Da), six PIO structure-related metabolite ions (M1-M6) that were not identified by MDF could be identified by our approach (Fig. 4). These results indicated that our approach could identify not only common metabolites identified by MDF but also some uncommon metabolite ions.

4. Conclusions

During the drug discovery process, developing a metabolomics-based data analysis approach for rapid drug metabolite identification is essential. A two-stage data analysis approach was developed for identifying PIO metabolite ions. We combined a time-course experiment with stable isotope tracing to mine data on possible PIO metabolite ions. This approach could effectively identify 25 isotope pairs from a complex matrix. A high ratio of ions (18/25) indicated a dose-response relationship. Most ions (14/18) could be verified as PIO structure-related metabolite ions. We also proved that our approach

could be used to identity PIO metabolites. Our approach could be used to mine not only common PIO metabolite ions that were identified by MDF but also uncommon PIO metabolite ions. However, some PIO metabolite ions identified using the OPLS-DA could not be identified using our approach. Differences in the design of metabolomics-based data analysis approaches could result in differences in the metabolite identification. In the future, a more comprehensive approach should be devised to identify all probable drug metabolites.

Funding

Declaration of competing interest

The authors declare no competing financial interests.

Acknowledgements

References

[1] Kostiainen R, Kotiaho T, Kuuranne T, Auriola S. Liquid chromatography/atmospheric pressure ionization-mass spectrometry in drug metabolism studies. J Mass Spectrom : JMS 2003;38:357—72. [In eng].

[2] Tautenhahn R, Böttcher C, Neumann S. Highly sensitive feature detection for high resolution LC/MS. BMC Bioinf 2008;9:504.

[3] Zhang H, Zhang D, Ray K, Zhu M. Mass defect filter technique and its applications to drug metabolite identification by high-resolution mass spectrometry. J Mass Spectrom : JMS 2009;44:999—1016. [In eng].

[4] Shih CL, Liao PM, Hsu JY, Chung YN, Zgoda VG, Liao PC. Identification of urinary biomarkers of exposure to di-(2-propylheptyl) phthalate using high-resolution mass spectrometry and two data-screening approaches. Chemosphere 2018;193:170—7. [In eng].

[5] Shih C-L, Wu H-Y, Liao P-M, Hsu J-Y, Tsao C-Y, Zgoda VG, et al. Profiling and comparison of toxicant metabolites in hair and urine using a mass spectrometry-based metabolomic data processing method. Anal Chim Acta 2019;1052:84—95.

[6] Geng J, Xiao L, Chen C, Wang Z, Xiao W, Wang Q. An integrated analytical approach based on enhanced fragment ions interrogation and modified Kendrick mass defect filter data mining for in-depth chemical profiling of glucosinolates

by ultra-high-pressure liquid chromatography coupled with Orbitrap high resolution mass spectrometry. J Chromatogr A 2021;1639:461903. [In eng].

[7] Domingo-Almenara X, Siuzdak G. Metabolomics data processing using XCMS. Methods Mol Biol 2020;2104:11—24. [In eng].

[8] Roosendaal J, Rosing H, Beijnen JH. Combining isotopic tracer techniques to increase efficiency of clinical pharmacokinetic trials in oncology. Drugs R 2020;20:147—54.

[9] Cui X, Zhang L, Su G, Kijlstra A, Yang P. Specific sweat metabolite profile in ocular Behcet's disease. Int Immunopharm 2021;97:107812. [In eng].

[10] de Campos ML, Padilha EC, Peccinini RG. A review of pharmacokinetic parameters of metabolites and prodrugs. Drug Metabol Lett 2014;7:105—16. [In eng].

[11] Hsu JY, Hsu JF, Chen YR, Shih CL, Hsu YS, Chen YJ, et al. Urinary exposure marker discovery for toxicants using ultra-high pressure liquid chromatography coupled with Orbitrap high resolution mass spectrometry and three untargeted metabolomics approaches. Anal Chim Acta 2016;939:73—83. [In eng].

[12] Hsu J-F, Peng L-W, Li Y-J, Lin L-C, Liao P-C. Identification of di-isononyl phthalate metabolites for exposure marker discovery using in vitro/in vivo metabolism and signal mining strategy with LC-MS data. Anal Chem 2011;83: 8725—31.

[13] Su C-Y, Wang J-H, Chang T-Y, Shih C-L. Mass defect filter technique combined with stable isotope tracing for drug metabolite identification using high-resolution mass spectrometry. Anal Chim Acta 2022. 1208:339814. [In eng].

[14] Li X, Yin M, Gu J, Hou Y, Tian F, Sun F. Metabolomic profiling of plasma samples from women with recurrent spontaneous abortion. Med Sci Mon 2018;24:4038—45. [In eng].

[15] Zhao S, Liu H, Su Z, Khoo C, Gu L. Identifying cranberry juice consumers with predictive OPLS-DA models of plasma metabolome and validation of cranberry juice intake biomarkers in a double-blinded, randomized, placebo-controlled, cross-over study. Mol Nutr Food Res 2020;64: e1901242. [In eng].

[16] Skorupa A, Poński M, Ciszek M, Cichoń B, Klimek M, Witek A, et al. Grading of endometrial cancer using (1)H HR-MAS NMR-based metabolomics. Sci Rep 2021;11:18160. [In eng].

[17] Hanefeld M. Pharmacokinetics and clinical efficacy of pioglitazone. Int J Clin Pract Symp Suppl 2001:19—25. [In eng].

[18] Maeda K. Hepatocellular injury in a patient receiving pioglitazone. Ann Intern Med 2001;135:306. [In eng].

[19] Marcy TR, Britton ML, Blevins SM. Second-generation thiazolidinediones and hepatotoxicity. Ann Pharmacother 2004;38:1419—23. [In eng].

[20] Chase MP, Yarze JC. Pioglitazone-associated fulminant hepatic failure. Am J Gastroenterol 2002;97:502—3. [In eng].

[21] Kassahun K, Pearson PG, Tang W, McIntosh I, Leung K, Elmore C, et al. Studies on the metabolism of troglitazone to reactive intermediates in vitro and in vivo. Evidence for novel biotransformation pathways involving quinone methide formation and thiazolidinedione ring scission. Chem Res Toxicol 2001;14:62—70.

[22] Shen Z, Reed JR, Creighton M, Liu DQ, Tang YS, Hora DF, et al. Identification of novel metabolites of pioglitazone in rat and dog. In: Xenobiotica; the fate of foreign compounds in biological systems. 33; 2003. p. 499—509. [In eng].

[23] Baughman TM, Graham RA, Wells-Knecht K, Silver IS, Tyler LO, Wells-Knecht M, et al. Metabolic activation of pioglitazone identified from rat and human liver microsomes and freshly isolated hepatocytes. Drug Metabol Dispos: the biological fate of chemicals 2005;33:733—8. [In eng].

[24] Hsu JF, Tien CP, Shih CL, Liao PM, Wong HI, Liao PC. Using a high-resolution mass spectrometry-based metabolomics strategy for comprehensively screening and identifying biomarkers of phthalate exposure: method development and application. Environ Int 2019;128:261—70. [In eng].

[25] Allen F, Pon A, Wilson M, Greiner R, Wishart D. CFM-ID: a web server for annotation, spectrum prediction and metabolite identification from tandem mass spectra. Nucleic Acids Res 2014;42:W94—9. [In eng].

[26] Tkalec Ž, Negreira N, López de Alda M, Barceló D, Kosjek T. A novel workflow utilizing open-source software tools in the environmental fate studies: the example of imatinib biotransformation. Sci Total Environ 2021;797:149063. [In eng].

[27] Schymanski EL, Jeon J, Gulde R, Fenner K, Ruff M, Singer HP, et al. Identifying small molecules via high resolution mass spectrometry: communicating confidence. Environ Sci Technol 2014;48:2097—8.

[28] Eriksson Ej L, Kettaneh-Wold N, Trygg CWJ, Wold aS. Multi- and megavariate data analysis: basic principles and applications. 2nd ed. Umea: Umetrics AB; 2006. p. 2006.

[29] Campos ML, Cerqueira LB, Silva BCU, Franchin TB, Galdino-Pitta MR, Pitta IR, et al. New pioglitazone metabolites and absence of opened-ring metabolites in new N-substituted thiazolidinedione. Drug Metabol Dispos: the biological fate of chemicals 2018;46:879—87. [In eng].

[30] Uchiyama M, Fischer T, Mueller J, Oguchi M, Yamamura N, Koda H, et al. Identification of novel metabolic pathways of pioglitazone in hepatocytes: N-glucuronidation of thiazolidinedione ring and sequential ring-opening pathway. Drug Metabol Dispos: the biological fate of chemicals 2010;38: 946—56. [In eng].

[31] Anari MR, Sanchez RI, Bakhtiar R, Franklin RB, Baillie TA. Integration of knowledge-based metabolic predictions with liquid chromatography data-dependent tandem mass spectrometry for drug metabolism studies: application to studies on the biotransformation of indinavir. Anal Chem 2004;76: 823—32. [In eng].

[32] Ma S, Chowdhury SK. Analytical strategies for assessment of human metabolites in preclinical safety testing. Anal Chem 2011;83:5028—36.

[33] Tanis SP, Parker TT, Colca JR, Fisher RM, Kletzein RF. Synthesis and biological activity of metabolites of the antidiabetic, antihyperglycemic agent pioglitazone. J Med Chem 1996;39:5053—63.